MAGNETO-HYDRODYNAMIC CHARACTERISTICS FOR WIDE SECANT-SHAPED SLIDER BEARINGS

Jaw-Ren Lin*, Hsiu-Lu Chiang, Rong-Fang Lu, Tsu-Liang Chou

Department of Mechanical Engineering, Nanya Institute of Technology

Abstract

In the present paper, the steady load-carrying capacity and the dynamic stiffness and damping coefficients of wide secant-shaped slider bearings using an electrically conducting fluid have been analyzed. By the application of externally transverse magnetic fields, an analytic-form solution for the magneto-hydrodynamic (MHD) secant-shaped slider bearing characteristics is obtained. In order to provide more information in slider bearing characteristics, the results are compared with the MHD inclined slider bearing. In addition, a numerical example for the MHD secant-shaped slider bearing characteristics is also included in Tables for industrial application.

Key Words: secant-shaped bearings, slider bearings, magneto-hydrodynamic characteristics

*Email: jrlin@nanya.edu.tw Tel: 03-4361070#6302 Fax: 03-4384670

正割形狀寬滑塊軸承之磁液動性能

林昭仁* 江新祿 盧榮芳 周祖亮

南亞技術學院 機械工程系

摘要

本文主要在探討電導流體為潤滑劑之正割形狀寬滑塊軸承之磁液動負荷性能、剛度性能以及阻尼性能。在外加磁場之作用下，本文導出推導得到正割形狀寬滑塊軸承磁液動性能之解析解。為能提供滑塊軸承性能之更多參考訊息，所得結果亦將與傾斜平面形狀寬滑塊軸承之磁液動性能作一比較。除此之外，本文亦提供磁液動正割形狀滑塊軸承之實例以及計算之性能數據，以利於工程師在工業上之參考與應用。

關鍵詞: 正割形狀滑塊，滑塊軸承，磁液動性能

1. Introduction

Traditionally, studies of lubrication characteristics of slider bearings focus upon the hydrodynamic mechanisms lubricated with non-conducting lubricants (NCL). Representative articles can be observed in the works by Cameron [1], Fuller [2], Hamrock [3], Lin and Hung [4] and Lu *et al.* [5]. Advanced researches considering further factors are carried out, such as the effects of fluid inertia by King and Taylor [6]; the effects of power-law lubricants by Wang and Jin [7], the effects of surface roughness by Wang and Li [8], and the effects of porous material by Lin [9]. To provide better characteristics, the application of electrically conducting liquid-metal fluids as lubricants by the application of magnetic fields has received a great attention. Therefore, many researches about the magneto-hydrodynamic (MHD) characteristics of thin-film bearings lubricated with an electrically conducting fluid by applying the externally magnetic fields have been carried out. Representative articles can be found in the MHD externally pressurized porous thrust bearings by Shukla [10]; the MHD circular and annular squeeze-film bearings by Soundalgekar and Amrute [11] and Lu *et al.* [12]; the MHD steady-state journal bearings by Sasada *et al.* [13] and Malik and Singh [14]; and the steady MHD slider bearings by Huges [15] and Soundalgekar [16]. Recently, the dynamic characteristics of a MHD inclined slider bearing have been analyzed by Lin *et al.* [17]. In order to provide more information in bearing selection and designing, we are motivated to study further the steady and dynamic characteristics of MHD slider bearings with a secant-shaped film profile.

On the basis of the MHD lubrication theory together with the application of externally magnetic field, the present study is mainly concerned with the steady load-carrying capacity and dynamic stiffness and damping characteristics of wide secant-shaped slider bearings lubricated with an electrically conducting fluid. An analytic-form solution for the secant-shaped slider bearing characteristics is obtained. Compared with the MHD inclined slider bearing, the steady load-carrying capacity and dynamic stiffness and damping coefficients of wide MHD secant-shaped slider bearings are presented for different values of the parameters. An illustrated example for the MHD secant-shaped slider bearing characteristics is also included for industrial application.

2. Analysis of MHD secant-shaped slider bearing characteristics

Figure 1 shows the physical configuration of a wide MHD secant-shaped slider bearing lubricated with a conducting incompressible fluid with electrical conductivity σ under the application of a z–direction magnetic field B_0. The inlet film thickness at the position $x = 0$:

$$h_1(t) = h_m(t) + \Delta \cdot h_m(t) = (\Delta + 1) \cdot h_m(t) \tag{1}$$

In this equation, $h_m(t)$ denotes the minimum film thickness at the outlet $x = L$, and Δ defines a non-dimensional profile parameter measured under steady state:

$$\Delta = \frac{h_{1s} - h_{ms}}{h_{ms}} \tag{2}$$

where the subscript s denotes the steady state, h_{1s} is the steady maximum film height at the inlet and h_{ms} is the steady minimum film height at the outlet. For this secant-shaped slider bearing, the film thickness can be described by:

$$h(x,t) = h_m(t) \cdot \sec\left[a \cdot \left(1 - x/L\right)\right] \tag{3}$$

$$a = \sec^{-1}(\Delta + 1) \tag{4}$$

Based upon the magneto-hydrodynamic thin-film lubrication theory, the non-dimensional MHD dynamic Reynolds-type equation for a slider bearing has been derived by Lin *et al.* [17]:

$$\frac{\partial}{\partial x^*}\left[A^*(Hn, h^*)\frac{\partial p^*}{\partial x^*}\right] = 6\frac{\partial h^*}{\partial x^*} + 12V^* \tag{5}$$

where $p^* = p{h_{ms}}^2/\eta UL$ denotes the non-dimensional MHD film pressure, $Hn = B_0 h_{ms}(\sigma/\eta)^{1/2}$ is the Hartmann number, $h^* = h/h_{ms}$ is the non-dimensional film thickness, $V^* = d{h_m}^*/d\tau$ is the non-dimensional squeezing velocity, $x^* = x/L$ is the non-dimensional coordinate, $\tau = Ut/L$ is the non-dimensional time, and $A^* = A/{h_{ms}}^3$ is the non-dimensional function defined by:

$$A^*(Hn, h^*) = \frac{6h^*}{Hn^2}\left[Hn \cdot h^* \coth(0.5Hn \cdot h^*) - 2\right] \tag{6}$$

For the secant-shaped slider bearing considered in this study, the non-dimensional film thickness is expressed by:

$$h^*(x^*, t^*) = {h_m}^*(t^*) \cdot \sec\left[a \cdot \left(1 - x^*\right)\right] \tag{7}$$

Solving the non-dimensional MHD dynamic Reynolds-type equation using the zero boundary conditions at the inlet and outlet positions, we can obtain the non-dimensional MHD film pressure. Integrating the MHD film pressure over the lubricant area results in the non-dimensional MHD film film force, $F^* = F^*({h_m}^*, V^*)$. Setting the non-dimensional MHD film force under the steady state "s" resulting the non-dimensional MHD steady

load-carrying capacity, $W_s^* = (F^*)_s$. By evaluating the partial derivative of MHD film force with respect to the minimum film thickness and setting the resulting terms under steady state, one can obtain the non-dimensional MHD dynamic stiffness coefficient, $K_d^* = -\left(\partial F^* / \partial h_m^*\right)_s$. By evaluating the partial derivative of MHD film force with respect to the squeezing velocity and setting the resulting terms under steady state, one can obtain the non-dimensional MHD dynamic damping coefficient, $D_d^* = -\left(\partial F^* / \partial V^*\right)_s$. After performing these procedures, we can derive an analytic-form solution of the MHD steady load-carrying capacity, the MHD dynamic stiffness coefficient, and the MHD dynamic damping coefficient:

$$W_s^* = 6 \cdot h_{ms}^* \cdot G_A(h_{ms}^*) + \alpha_{1s} \cdot G_C(h_{ms}^*) \tag{8}$$

$$K_d^* = -6 \cdot G_A(h_{ms}^*) - 6 \cdot h_{ms}^* \cdot \left(\frac{\partial G_A}{\partial h_m^*}\right)_s - G_C(h_{ms}^*) \cdot \left(\frac{\partial \alpha_1}{\partial h_m^*}\right)_s - \alpha_{1s} \cdot \left(\frac{\partial G_C}{\partial h_m^*}\right)_s \tag{9}$$

$$D_d^* = -12\left[G_B(h_{ms}^*) - G_C(h_{ms}^*) \cdot \frac{g_{B1}(h_{ms}^*)}{g_{C1}(h_{ms}^*)}\right] \tag{10}$$

In these equations the related functions are defined in **Appendix A**.

3. Results and discussion

MHD secant-shaped bearing characteristics. Figure 2 shows the non-dimensional MHD steady load-carrying capacity W_s^* as a function of the Hartmann number Hn for different values of the profile parameter Δ at the steady minimum film thickness, $h_{ms}^* = 0.5$. For the secant-shaped bearing under $\Delta = 1.0$, the steady load-carrying capacity is observed to increase with increasing values of Hn. Increasing the profile parameter up to $\Delta = 2.0$ increases the steady load-carrying capacity of the bearing especially for larger values of Hn that resulting from the externally applied magnetic fields. Comparing with the MHD inclined-plane bearing, the MHD secant-shaped bearing provides higher load capacity under larger values of the Hartmann number and the profile parameter. Figure 3 presents the non-dimensional MHD dynamic stiffness coefficient K_d^* as a function of the Hartmann number Hn for different values of the profile parameter Δ at the steady minimum film thickness, $h_{ms}^* = 0.5$. For the secant-shaped bearing designed under the profile parameter $\Delta = 1.0$, the dynamic stiffness coefficient increases smoothly with the values of the Hartmann number. Increasing the profile parameter up to $\Delta = 2.0$ increases the dynamic stiffness coefficient of the secant-shaped bearing. Comparing with the MHD inclined-plane bearing, the MHD secant-shaped bearing is observed to result in higher values of the

dynamic stiffness coefficient especially for the bearing operating under larger values of Hn and Δ. Figure 4 describes the non-dimensional MHD dynamic damping coefficient D_d^* as a function of the Hartmann number Hn for different values of the profile parameter Δ at the steady minimum film thickness, $h_{ms}^* = 0.5$. For the secant-shaped bearing, the dynamic damping coefficient is observed to increases with the values of the Hartmann number. Comparing with the MHD inclined-plane bearing, the MHD secant-shaped bearing is seen to provide higher values of the dynamic damping coefficient especially for the bearing operating under larger values of the Hartmann number.

Numerical example. For industrial application, a numerical example of the secant-shaped slider bearing lubricated with an electrically conducting fluid is illustrated in Table 1; these data are modified from Lin *et al.* [17] in the study of MHD inclined-plane slider bearing. Based upon the present analysis, the profile parameter Δ and the Hartmann number Hn of the MHD secant-shaped slider bearing can be evaluated:

$\Delta = (h_{1s} - h_{ms}) / h_{ms} = 0.5,\ 1.0,\ 1.5,\ 2.0,\ 2.5$; and

$Hn = B_0 h_{ms} (\sigma / \eta)^{1/2} = 0,\ 1.97,\ 3.94,\ 5.91,\ 7.88,\ 9.85$

By the expressions in equations (8), (9) and (10), the MHD steady load-carrying capacity, the MHD dynamic stiffness coefficient and the MHD dynamic damping coefficient are predicted and then presented in Table 2; in Table 2, the results of the NCL secant-shaped slider bearing by Lu *et al.* [5] are also included for the comparison. It is found that under the limiting case: $Hn = 0$, the calculated results of the present analysis agree well with the NCL secant-shaped slider bearing by Lu *et al.* [5]. This comparison shows an agreeing support of the present analysis.

4. Conclusions

Using an electrically conducting fluid as the lubricant, the steady load-carrying capacity and the dynamic coefficients of wide secant-shaped slider bearings under the application of transverse magnetic fields are presented. Based upon the above analysis and results, we can draw the following conclusions.

An analytic-form solution for the MHD secant-shaped slider bearing is obtained and applied to evaluate bearing characteristics. Comparing with the NCL secant-shaped slider bearing by Lu *et al.* [5], the MHD secant-shaped slider bearing signifies an improvement in the steady load, the dynamic stiffness coefficient and the dynamic

damping coefficient. Comparing with the MHD inclined-plane bearing by Lin *et al.* [17] the MHD secant-shaped bearing provides higher dynamic damping coefficients, especially for the secant-shaped bearing operating under larger Hartmann numbers.

References

1. Cameron, A., Basic Lubrication Theory, Longmans Green & Co Ltd, London (1966).
2. Fuller, D.D., Theory and Practice of Lubrication for Engineers, John Wiley and Sons, New York (1984).
3. Hamrock, B.J., Fundamentals of Fluid Film Lubrication, McGraw Hill Inc., New York (1994).
4. Lin, J.R., and Hung, C.R., "Analysis of Dynamic Characteristics for Wide Slider Bearings with an Exponential Film Profile," Journal of Marine Science and Technology, Vol. 12, pp. 217-221 (2004).
5. Lu, R.F., Liao, W.H., and Lin, J. R., "Analysis of Dynamic Characteristics of Wide Secant Shaped Slider Bearing," The 27th Conference on Theoretical and Applied Mechanics, Tainan, Taiwan, ROC (2003).
6. King, K.F., and Taylor, C.M., "An Estimation of the Fluid Inertia on the Performance of the Inclined Slider Thrust Bearing with Particular Regard to Turbulent Lubrication," ASME Journal of Lubrication Technology, Vol. 99, pp. 129-135 (1997).
7. Wang, J., and Jin, G., "The Optimal Design of the Rayleigh Slider Bearings with a Power-law Fluid," Wear, Vol. 129, pp. 1-11 (1989).
8. Wang, J., and Li, B., "The Effects of Rheological Characteristics of Lubricant and Surface Roughness on the Load Capacity of a Hydrodynamic Slider Bearing," Wear, Vol. 146, pp. 165-177 (1991).
9. Lin, J.R., "Optimal Design of One-dimensional Porous Slider Bearings Using the Brinkman Model," Tribology International, Vol.34, pp.57-64 (2001).
10. Shukla, J.B., "Magnetohydrodynamic Externally Pressurized Porous Thrust Bearings," Wear, Vol. 63, pp. 149-157 (1980).
11. Soundalgekar, V.M., and Amrute, A.S., "Effects of External Circuit on MHD Squeeze Film between Conducting Plates," Wear 19, pp. 117-122 (1972).
12. Lu, R.F., Chien, R.D., and Lin, J.R., "Effects of Fluid Inertia in Magneto-hydrodynamic Annular Squeeze Films," Tribology International, Vol. 39,

pp. 221-226 (2006).

13. Sasada, T., Kurosaki, Y., Honda, K., and Kamijo, K., "MHD Journal Bearing in a Magnetic Field Perpendicular to Its Axis (1st Report, Analysis of an Infinitely Long Bearing)," Bulletin of the JSME, vol. 17, pp. 1645-1651 (1974).
14. Malik, M., and Singh, D.V., "Analysis of Finite Magnetohydrodynamic Journal Bearings," Wear, Vol. 64, pp. 273-280 (1980).
15. Huges, W.F., "The Magnetohydrodynamic Inclined Slider Bearing with a Transverse Magnetic Field," Wear, Vol. 6, pp. 315-324 (1963).
16. Soundalgekar, V.M., "Effects of an External Circuit on a MHD Slider Bearing," Wear, Vol. 21, pp. 17-25 (1972).
17. Lin, J.R., Hung, C.R., Hsu, C.H., and Chuan, L., "Dynamic Stiffness and Damping Characteristics of One-dimensional Magneto-hydrodynamic Inclined-plane Slider Bearings," P I MECH ENG J-J TRIB, Vol. 223, pp. 211-219 (2009).

Appendix A: The related functions

$$g_A(h_m^*, x^*) = \int_{x^*=0}^{x^*} \frac{\sec\left[a \cdot \left(1 - x^*\right)\right]}{A^*(Hn, h^*)} dx^* \tag{A.1}$$

$$g_B(h_m^*, x^*) = \frac{-1}{a} \cdot \int_{x^*=0}^{x^*} \frac{\ln\left\{\tan\left[0.5a(1 - x^*) + \pi/4\right]\right\}}{A^*(Hn, h^*)} dx^* \tag{A.2}$$

$$g_C(h_m^*, x^*) = \int_{x^*=0}^{x^*} \frac{1}{A^*(Hn, h^*)} dx^* \tag{A.3}$$

$$g_{A1} = \int_{x^*=0}^{1} \frac{\sec\left[a \cdot \left(1 - x^*\right)\right]}{A^*(Hn, h^*)} dx^* \tag{A.4}$$

$$g_{B1} = \frac{-1}{a} \cdot \int_{x^*=0}^{1} \frac{\ln\left\{\tan\left[0.5a(1 - x^*) + \pi/4\right]\right\}}{A^*(Hn, h^*)} dx^* \tag{A.5}$$

$$g_{C1} = \int_{x^*=0}^{1} \frac{1}{A^*(Hn, h^*)} dx^* \tag{A.6}$$

$$G_A(h_m{}^*) = \int_{x^*=0}^{1} \int_{x^*=0}^{x^*} \frac{\sec\left[a \cdot \left(1 - x^*\right)\right]}{A^*(Hn, h^*)} dx^* dx^* \tag{A.7}$$

$$G_B(h_m{}^*) = \frac{-1}{a} \cdot \int_{x^*=0}^{1} \int_{x^*=0}^{x^*} \frac{\ln\left\{\tan\left[0.5a(1 - x^*) + \pi/4\right]\right\}}{A^*(Hn, h^*)} dx^* dx^* \tag{A.8}$$

$$G_C(h_m{}^*) = \int_{x^*=0}^{1} \int_{x^*=0}^{x^*} \frac{1}{A^*(Hn, h^*)} dx^* dx^* \tag{A.9}$$

$$\alpha_{1s} = -6 \cdot \frac{(g_{A1})_s}{(g_{C1})_s} \tag{A.10}$$

$$\frac{\partial g_{A1}}{\partial h_m^*} = -\int_{x^*=0}^{1} \frac{\sec\left[a\cdot\left(1-x^*\right)\right]}{A^{*2}(Hn,h^*)} \frac{\partial A^*}{\partial h_m^*} dx^* \tag{A.11}$$

$$\frac{\partial g_{C1}}{\partial h_m^*} = -\int_{x^*=0}^{1} \frac{1}{A^{*2}(Hn,h^*)} \frac{\partial A^*}{\partial h_m^*} dx^* \tag{A.12}$$

$$\frac{\partial G_A}{\partial h_m^*} = -\int_{x^*=0}^{1}\int_{x^*=0}^{x^*} \frac{\sec\left[a\cdot\left(1-x^*\right)\right]}{A^{*2}(Hn,h^*)} \cdot \frac{\partial A^*}{\partial h_m^*} dx^* dx^* \tag{A.13}$$

$$\frac{\partial G_C}{\partial h_m^*} = -\int_{x^*=0}^{1}\int_{x^*=0}^{x^*} \frac{1}{A^{*2}(Hn,h^*)} \cdot \frac{\partial A^*}{\partial h_m^*} dx^* dx^* \tag{A.14}$$

$$\frac{\partial \alpha_1}{\partial h_m^*} = \frac{-6}{g_{C1}^{\ 2}} \cdot \left[\left(g_{A1} + h_m^{\ *} \cdot \frac{\partial g_{A1}}{\partial h_m^*}\right) \cdot g_{C1} - h_m^{\ *} \cdot g_{A1} \cdot \frac{\partial g_{C1}}{\partial h_m^*}\right] \tag{A.15}$$

$$\frac{\partial A^*}{\partial h_m^*} = \frac{3\cdot\sec\left[a\cdot\left(1-x^*\right)\right]}{Hn^2} \cdot \begin{bmatrix} 4Hn\cdot h^* \coth(0.5Hn\cdot h^*) \\ -Hn^2\cdot h^{*2}\cdot \csc h^2(0.5Hn\cdot h^*) - 4 \end{bmatrix} \tag{A.16}$$

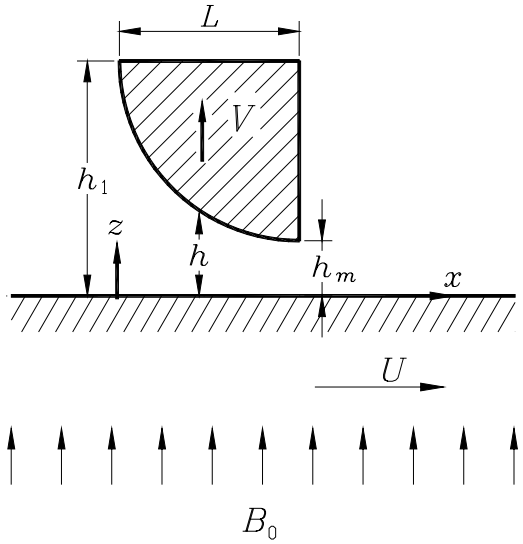

Figure 1 Physical configuration of the wide MHD secant-shaped slider bearing

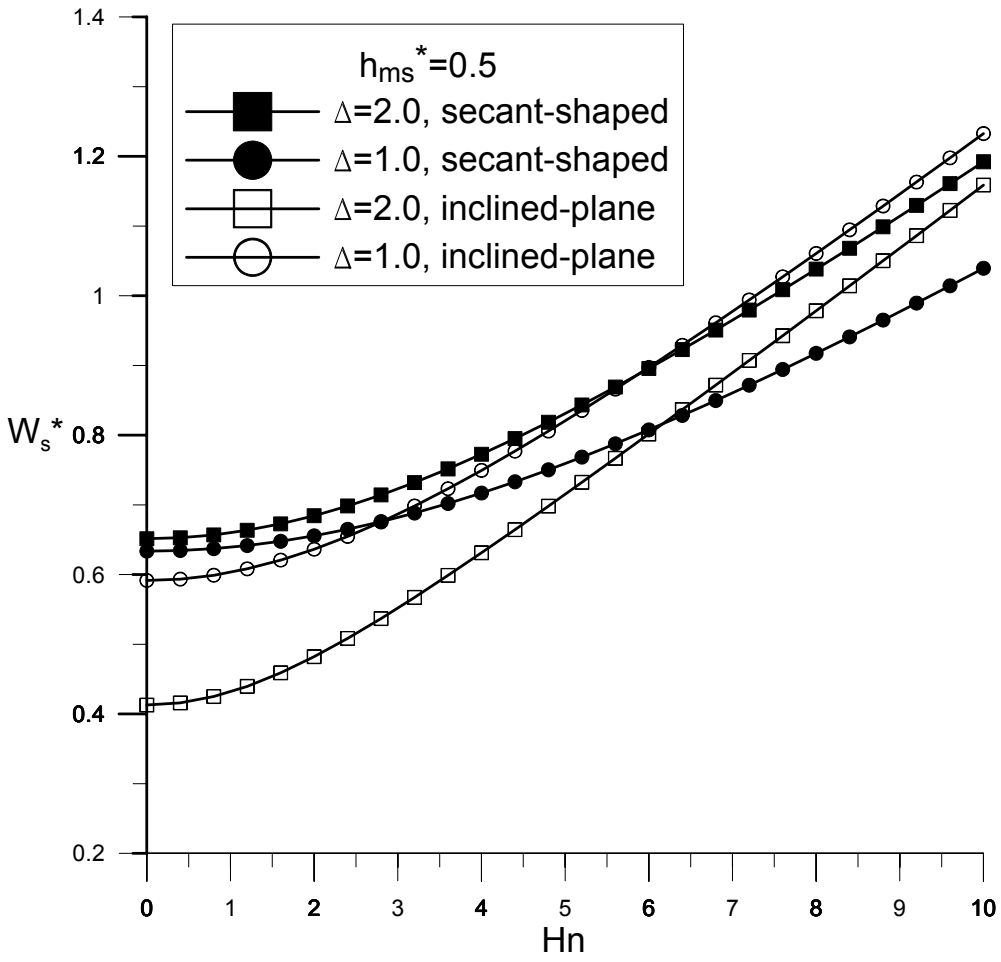

Figure 2 MHD steady load-carrying capacity W_s^* as a function of Hn

for different Δ at $h_{ms}^* = 0.5$

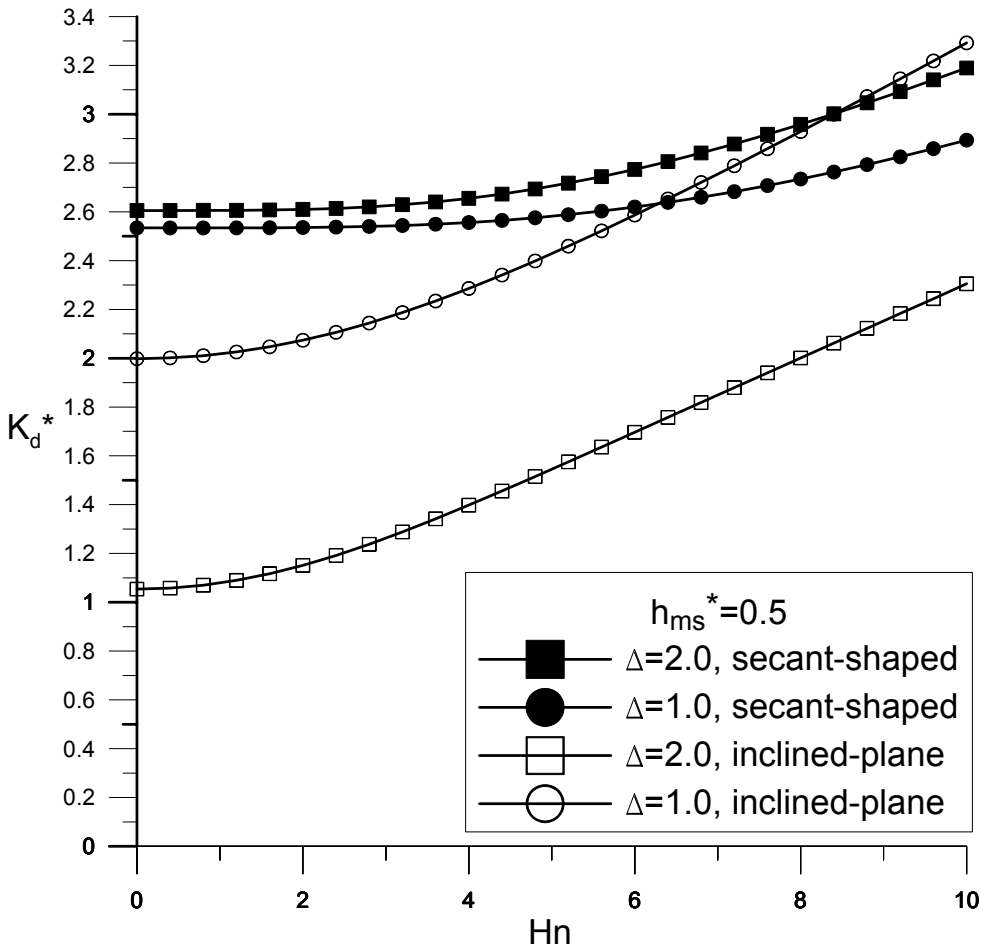

Figure 3 MHD dynamic stiffness coefficient K_d^* as a function of Hn

for different Δ at $h_{ms}^* = 0.5$

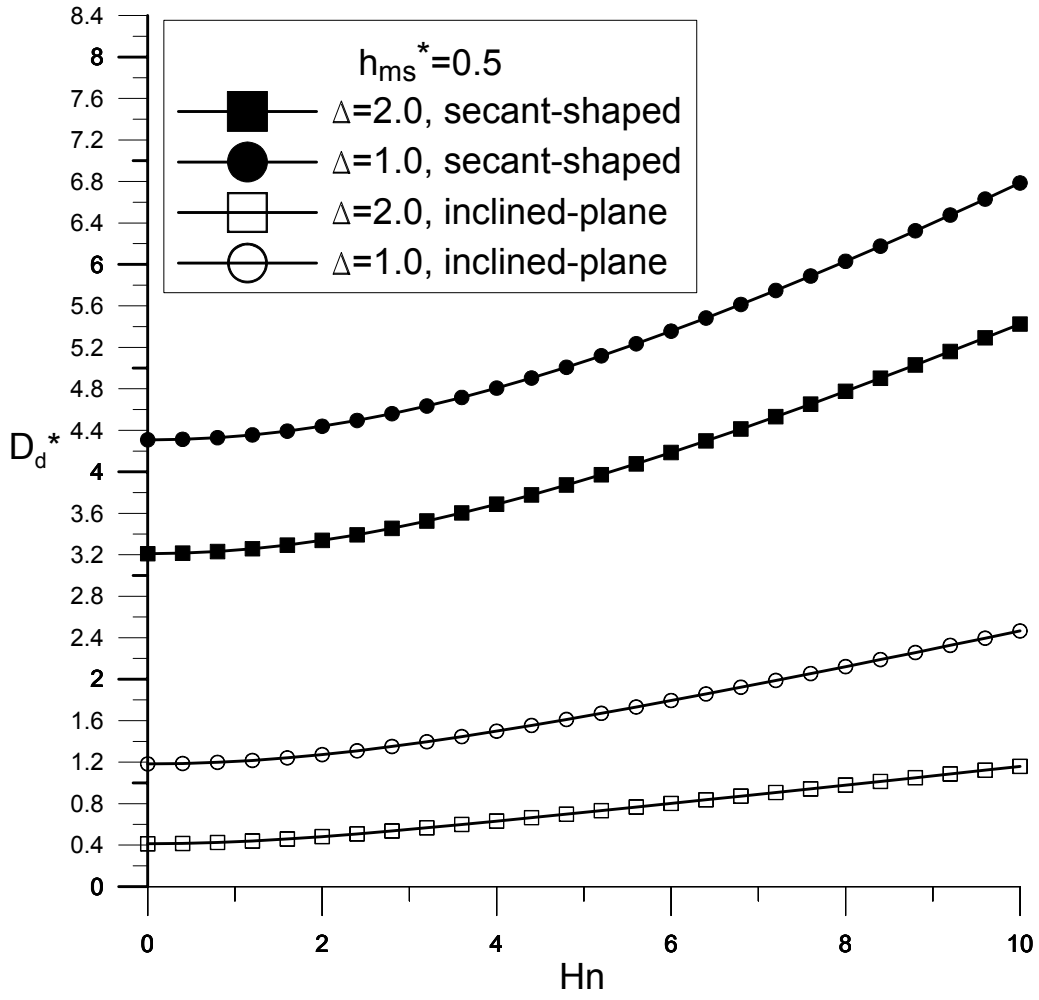

Figure 4 MHD dynamic damping coefficient D_d^* as a function of Hn

for different Δ at $h_{ms}^* = 0.5$

Table 1 Illustration of the MHD secant-shaped slider bearings

Data of the MHD secant-shaped slider bearing		
Inlet-outlet thickness difference	$h_{1s} - h_{ms}$	$(0.25,\ 0.50,\ 0.75,\ 1.00,\ 1.25)\times 10^{-4}\ \ m$
Steady minimum film thickness	h_{ms}	$0.50\times 10^{-4}\ \ m$
Lubricant viscosity	η	$1.55\times 10^{-3}\ \ Pa\cdot s$
Electrical conductivity	σ	$1.07\times 10^{6}\ mho/m$
Applied magnetic field	B_0	$0,\ 1.50,\ 3.00,\ 4.50,\ 6.00,\ 7.50\ \ Wb/m^2$

Table 2 MHD secant-shaped bearing characteristics W_s^*, K_d^*, D_d^* and comparison with the NCL secant-shaped bearing characteristics.

		Lu *et al.* [5]	Present study					
Characteristics	Δ	NCL	Hn =0	Hn =1.97	Hn =3.94	Hn =5.91	Hn =7.88	Hn =9.85
W_s^*	0.5	0.13	0.1287	0.1409	0.2724	0.2142	0.2607	0.3093
	1.0	0.16	0.1584	0.1787	0.2276	0.2893	0.3562	0.4254
	1.5	0.16	0.1640	0.1897	0.2487	0.3206	0.3973	0.4763
	2.0	0.16	0.1629	0.1924	0.2574	0.3346	0.4165	0.5005
	2.5	0.15	0.1600	0.1921	0.2607	0.3410	0.4257	0.5124
K_d^*	0.5	0.26	0.2574	0.2585	0.2690	0.2941	0.3301	0.3723
	1.0	0.32	0.3168	0.3194	0.3408	0.3836	0.4391	0.5014
	1.5	0.33	0.3279	0.3322	0.3625	0.4162	0.4821	0.5544
	2.0	0.33	0.3257	0.3316	0.3683	0.4286	0.5002	0.5779
	2.5	0.32	0.3199	0.3272	0.3685	0.4327	0.5077	0.5883
D_d^*	0.5	0.69	0.6902	0.7518	0.9110	1.1245	1.3635	1.6144
	1.0	0.54	0.5385	0.5992	0.7485	0.9402	1.1503	1.3690
	1.5	0.45	0.4537	0.5132	0.6537	0.8293	1.0196	1.2167
	2.0	0.40	0.4013	0.4593	0.5925	0.7560	0.9321	1.1141
	2.5	0.37	0.3662	0.4229	0.5500	0.7043	0.8700	1.0409